Journal Pre-proofs

The Role of Artificial Intelligence in Generating Original Scientific Research

Moe Elbadawi, Hanxiang Li, Abdul W. Basit, Simon Gaisford

PII: S0378-5173(23)01163-8
DOI: https://doi.org/10.1016/j.ijpharm.2023.123741
Reference: IJP 123741

To appear in: *International Journal of Pharmaceutics*

Received Date: 12 September 2023
Revised Date: 20 December 2023
Accepted Date: 22 December 2023

Please cite this article as: M. Elbadawi, H. Li, A.W. Basit, S. Gaisford, The Role of Artificial Intelligence in Generating Original Scientific Research, *International Journal of Pharmaceutics* (2024), doi: https://doi.org/10.1016/j.ijpharm.2023.123741

The Role of Artificial Intelligence in Generating Original Scientific Research

Moe Elbadawi[1,*], Hanxiang Li, Abdul W. Basit, Simon Gaisford[*]

UCL School of Pharmacy, University College London, 29-39 Brunswick Square, London, WC1N 1AX, UK

[1]Present address; School of Biological and Behavioural Sciences, Queen Mary University of London, Mile End Road, London E1 4DQ, UK

*Co-Corresponding authors

E-mail: s.gaisford@ucl.ac.uk

m.elbadawi@qmul.ac.uk

Abstract

Artificial intelligence (AI) is a revolutionary technology that is finding wide application across numerous sectors. Large language models (LLMs) are an emerging subset technology of AI and have been developed to communicate using human languages. At their core, LLMs are trained with vast amounts of information extracted from the internet, including text and images. Their ability to create human-like, expert text in almost any subject means they are increasingly being used as an aid to presentation, particularly in scientific writing. However, we wondered whether LLMs could go further, generating original scientific research and preparing the results for publication. We tasked GPT-4, an LLM, to write an original pharmaceutics manuscript, on a topic that is itself novel. It was able to conceive a research hypothesis, define an experimental protocol, produce photo-realistic images of printlets, generate believable analytical data from a range of instruments and write a convincing publication-ready manuscript with evidence of critical interpretation. The model achieved all this is less than 1h. Moreover, the generated data were multi-modal in nature, including thermal analyses, vibrational spectroscopy and dissolution testing, demonstrating multi-disciplinary expertise in the LLM. One area in which the model failed, however, was in referencing to the literature. Since the generated experimental results appeared believable though, we suggest that LLMs could certainly play a role in scientific research but with human input, interpretation and data validation. We discuss the potential benefits and current bottlenecks for realising this ambition here.

Key words: Pharmaceutical 3D Printing, Selective Laser Sintering, Artificial Intelligence, AI, Large Language Models

1. Introduction

Artificial intelligence (AI) is a ground-breaking technology that is driving advancements in both technology and society in many fields (Briganti and Le Moine, 2020; Palagi and Fischer, 2018; Wang et al., 2022b; Wang et al., 2023b). Its primary goal is to mimic human intelligence and, as a result, to carry out human tasks (Xu et al., 2021), but at a much faster pace than humans can achieve. This capability can solve challenges like workforce shortages and eliminates the need to expose humans to hazardous situations (Gao et al., 2021). In the drug discovery process, AI provides virtual simulations, which can significantly reduce the time needed for introducing new molecules to market (Chen et al., 2018; Das et al., 2021; Popova et al., 2018). This is invaluable given the escalating cost of developing products to commercial launch. Consequently, the pharmaceutical industry has begun to explore the applications of AI to product development (Elbadawi et al., 2021).

Machine learning (ML), a branch of AI, is instrumental in increasing the efficiency of complex processes, such as forecasting three dimensional (3D) printing capabilities (Elbadawi et al., 2020, Elbadawi et al, 2024), predicting drug-food interactions (Gavins et al., 2022; Kim et al., 2022), and modelling long-acting injectables (Bannigan et al., 2023). Another AI subset, machine vision (MV), is being used for tasks such as real-time monitoring of the disintegration of oral films, and is a key element in the application of process analytical technology (PAT) to tablet coating (Ficzere et al., 2022; Galata et al., 2021; O'Reilly et al., 2021; Rodrigues et al., 2021). Additionally, AI is helping the development of robotics by mimicking human movements effectively (Langer et al., 2019; von Erlach et al., 2020).

A less commonly used subset of AI, in pharmaceutics at least, is natural language processing (NLP), which aims to replicate human conversation, enhancing machine-human communication (Holler and Levinson, 2019; Trenfield et al., 2022). This allows enhanced access to machines and digital content, making the technology more accessible. Historically, interacting with machines primarily required coding, a skill not widely held. This barrier hindered researchers eager to harness the power of AI for solving pharmaceutical challenges. However, after years in development, a breakthrough in NLP was made by the development of large language models (LLMs), which has made NLP available to the masses. These models, with access to a vast number of data, deliver on-demand intelligent responses to questions posed by human users (Agathokleous et al., 2023; De Angelis et al., 2023). This is in stark contrast to the time needed for manual retrieval of information by sifting through published work. With the overwhelming surge in scientific publications, manually locating specific information has become an arduous task. For instance, answering a seemingly simple question like "how many types of 3D printing technologies exist?" can be challenging given the expanse and breadth of the pharmaceutical literature. This has left an unmet need in the 21st century for a more efficient means of extracting relevant information (Trewartha et al., 2022). Faster information retrieval in theory should result in faster discoveries and developments.

At their core, LLMs utilise neural networks trained on billions of words and images sourced from the internet, aiming to identify connections between them (Thirunavukarasu et al., 2023). During this process, the model learns patterns, facts, grammar and even how words and ideas relate to each other. Once trained, the model can generate its own text, answer questions, or help with tasks by drawing on a large pool of learned information, almost like recalling knowledge from a gigantic digital brain. In 2020, LLMs, like the generated pre-trained transformer (GPT), could execute tasks using minimal instructions (Floridi and Chiriatti, 2020). Since then, LLM technology has advanced such that they can understand multi-modal data, like sound and visual information and its uses now encompasses generating on-demand content such as text and images. Therefore, LLMs are categorised as generative AI models, distinguishing them from earlier studies that used ML primarily for predicting outcomes.

LLMs have shown promise in generating new content, especially in the medical field, by aiding in automating written tasks. For example, Kung et al. (2023) showcased how Chat-GPT can aid in clinical decision-making. In academia, some publications have credited LLMs as co-authors, highlighting their contribution to scientific literature, and most journals now require authors to declare any use of AI. LLMs have contributed to writing review articles and even crafting experimental procedures (Frye, 2022; Marquez et al., 2023; Norris, 2023; Rahimi and Talebi Bezmin Abadi, 2023). In plant science, they have been employed to pose 'key questions in plant science' (Agathokleous et al., 2023). However, to the best of our knowledge, LLMs have not yet written a data-driven, original research article from inception to publication. In fields like pharmaceutics, creating an original, hypothesis-driven research article with accompanying data and critical interpretation is a resource-intensive endeavour requiring expertise, skill, equipment, instrumentation and materials. If LLMs can handle such a task, they could revolutionise the research landscape. This would not only illustrate their capacity for information retrieval but also their potential to produce original content, surpassing tasks like literature review writing.

To that end, we tested an LLM, GPT-4, setting it the task of writing an original data-driven pharmaceutical research paper. We asked it to create a research hypothesis, generate the accompanying data to be discussed and write a submission-ready manuscript in the authors' field of expertise; 3D printing of medicines. 3D printing is an emerging technology in manufacturing medicines and has shown great potential for addressing the lack of personalised and precise medicines (Dedeloudi et al., 2023; Elbadawi et al., 2023; Englezos et al., 2023). The technology remains in its nascent phase, and thus there are relatively few data publicly available for training LLMs. We tasked the model with imagining how a tablet comprising paracetamol dispersed in PLGA with candurin would be fabricated with selective laser sintering (SLS) printing. PLGA was selected as the main excipient because its use in pharmaceutical SLA 3D printing has not previously been evaluated (and so no literature data were available to the LLM) and it is expensive (so evaluating its use

with AI potentially saves a lot of research cost). The AI-generated manuscript is appended at the end of the manuscript and we discuss our experience with GPT-4 in this report.

2. Experimental Procedure

Prompts (full details of which are appended in the supplementary information) were submitted to ChatGPT PLUS using the GPT-4 model (Chat-GPT July 20 Version). Text responses from prompts were copied and pasted into Word. To generate data, the model was prompted to generate representative code for python. The code was then ported to python (v3.11.1) and the plots generated were transferred to the manuscript. For image production, the application programming interface (API) supplied by OpenAI for python was used (openai v.0.27.8). Image generation was performed with the DALL-E model, which is a generative NLP model. Similar to GPT-4, the model was prompted with text and the generated images were copied and pasted into the manuscript.

3. Results and Discussion

GPT-4's ability to write an original manuscript, including within the text data, plots and images, was nothing short of remarkable. In less than one hour, the AI platform was able to generate the results of a study and prepare a manuscript for publication. In other words, the entire contents of the manuscript presented below were generated *de novo* by AI. While it may not be surprising that GPT-4 could generate the words to describe the data, the fact that it could generate data to support a research hypothesis is a key, and somewhat unexpected, finding.

Typically, users interact with GPT-4 through text, but our study has shown that LLMs can go further, and convert text into data, figures and images, all of which are common means of data representation in manuscripts. We chose to prompt the LLM with a drug and polymer combination (paracetamol with PLGA and a colourant dye, candurin) which had not been previously reported in the literature; hence, it was not possible for the LLM to simply retrieve data from the internet. It had to create data and images *de novo*.

Different types of data, including spectroscopic, optical and x-ray micro-computed tomography (XRMCT), were created and they looked compelling. Additionally, the model provided a critical commentary of the data. For example, it produced sensible glass transition and melting temperatures for PLGA and a melting temperature for paracetamol, and knew how these would manifest in a differential scanning calorimetry (DSC) thermogram (Table 1) (Lanao et al., 2013). Similarly, it produced prototypical degradation plots for these components and was able to simulate their thermal gravimetric analysis (TGA) curves (Awad et al., 2019; Giri and Maniruzzaman, 2022; Shi et al., 2018; Zhang et al., 2023). For human researchers,

this level of knowledge retrieval would require an exhaustive period of literature surveying, for each component, and matching that with experimental data.

Table 1. Features of the simulated TGA and DSC compared to real-world examples.

Characterisation Technique	Material	Feature	Reference
TGA	PLGA	Degradation onset ~300 °C, and complete degradation by 350 °C	(Jose et al., 2009)
	Paracetamol	Degradation onset ~ 250 °C and complete degradation by 300 °C	(de Oliveira et al., 2017; Goyanes et al., 2015)
	Candurin	Thermally stable until 500 °C, with minor weight loss	(Zhang et al., 2023)
DSC	PLGA	T_g at ~ 60 °C and T_m ~ 140 °C	(Walejewska et al., 2020)
	Paracetamol	T_m ~ 170 °C	(Khaled et al., 2018b)
	Candurin	No thermal events between 25 to 250 °C.	(Madžarević et al., 2021)

The simulated Fourier-transformed infrared (FTIR) spectra were particularly good. FTIR data typically require multi-variate analysis to interpret and is not a trivial task. Here, AI was able to work through it logically. First, it recalled the chemical structure of, for example, paracetamol. Thereafter, it postulated potential vibration bands based on the chemical structure of the material and how they would manifest themselves in an FTIR plot. As a result, the simulated FTIR plots were indistinguishable from real FTIR plots (Table 2). For XRD, GPT-4 was able to classify the materials as either crystalline, semi-crystalline or amorphous and was able to produce intensity peaks for each material (Table 2).

While the ability of the model to generate data was good, its ability to demonstrate critical thinking was even more impressive. For instance, it postulated an effect of laser scanning speed on the mechanical and dissolution properties of the printlets, even though there is no template or previous precedence for this in the literature. It also showed a relationship between laser speed and printlet porosity, and used this to explain differences in mechanical properties and dissolution profiles. Interestingly, its ability to analyse critically how paracetamol might become amorphous during SLS printing, and how this might alter DSC, FTIR and X-ray diffraction (XRD) data, demonstrate a fundamental understanding of both material and pharmaceutical sciences.

Table 2. Features of the simulated FTIR and XRD compared to real-world examples.

Characterisation Technique	Material	Feature	Reference
FTIR	PLGA	Characteristic single peak at 1750 cm^{-1} and multiple peaks between 1550 to 850 cm^{-1}	(Dou et al., 2021; Wei et al., 2022)
	Paracetamol	Characteristic band ~ 3200 cm^{-1} and multiple peaks between 1600 to 500 cm^{-1}	(Khaled et al., 2018a)
	Candurin	Characteristic peak ~ 1000 cm^{-1}	(Zhang et al., 2023)
XRD	PLGA	Semi-crystalline; few peaks	(Jeong et al., 2023)
	Paracetamol	Crystalline; multiple peaks	(Khaled et al., 2018a; Prasad et al., 2019)
	Candurin	Crystalline; few peaks	(Davis et al., 2020)

We also used AI's text-to-image feature to generate images of the printlets. While the main object (i.e. the printlet) was perfectly captured, the model can be seen to struggle with the surrounding content. In particular, the ruler hash marks can be seen to be abnormal. Minor abnormalities in photographic images like this are a key indicator that they are not real, and this may be an important tool in determining whether images are real or artificial.

The model was also tasked with generating X-ray Micro Computed Tomography (XRMCT) images. Here, the images showed printlets with a similar morphology to previous work (Fina et al., 2017), although improvements would be needed to make these images appear more realistic.

Finally, the ability of the model to write was also striking. Communicating the results of a study is a critical aspect of scientific research, and a lot of information can be embedded in text that cannot be otherwise communicated. In addition to the results section, GPT-4 was able to generate a methodology section, including within it some very detailed experimental protocols, similar to those noted by Marquez et al., (2023). The ability to create such detailed work plans may help guide researchers who are new to a particular discipline or technique, especially in today's cross-disciplinary environment. The model was also able to rationalise the need for the study and provided some background information in the Introduction.

There were two areas where the model showed any deficiencies. One was a lack of keywords, and the other was in referencing literature. Indeed, no references were cited and it is not clear why the model was unable to accomplish this. It may be that the model seeks data from the internet, assuming all information is not attributable to specific authors, and does not scan individual research papers, in the way that a human researcher would. Of course, many of the data the model generated were created de novo, and so could not be cited, but the lack of citations in the introduction section is a clear weakness, although this may be used as the basis of a method for identifying text that has been generated with AI.

Overall though, by showing an ability to write an original research article, AI has achieved a significant breakthrough in simulating human intelligence. The results of this study suggest that LLMs have the potential to transform pharmaceutical research radically, despite their infancy. The authors have been interested in using AI to automate aspects of the pharmaceutical research pipeline in the interest of accelerating discoveries and developments and doing so in an environmentally sustainable manner (Abdalla et al., 2023; McCoubrey et al., 2022; Wang et al., 2023a) and we have been successful in modelling and automating many aspects of the research pipeline. However, we have always needed the laborious steps of data collection and pre-processing of information to feed into an AI model. Here, in

contrast, no data collection or data pre-processing was needed; The LLM generated everything *de novo*, which allowed completion of its task at a fast pace.

We have not yet experimentally validated the outcomes of the model, by printing and characterising PLGA/paracetamol tablets but what has been achieved within this study builds on our previous work. For example, AI's ability to simulate FTIR data from simple text prompts is unprecedented and opens up new avenues of sustainable simulations and the prospect of simulating the entire research pipeline appears feasible. Further 'stress tests' are needed to see how LLMs can cope with human inter- and intra-variability, which are known to cause variability in data and has been an attributor of data irreproducibility. Indeed, other sources of variations, such as ambient temperature and humidity variation, should be factored in by LLM when generating simulated data, and it will be interesting to see how the platform can adapt to these unpredictable scenarios, as well as being integrated into Internet of Things (IoT) framework (Olvera and Monaghan, 2021; Raijada et al., 2021).

Its ability to write a manuscript on a research topic that itself is emerging was incredible. Relative to other pharmaceutical research topics, there is limited information surrounding SLS printing of medicines (Charoo et al., 2020). It is anticipated that as the knowledge of SLS develops, so too will AI's prowess of the topic. SLS printing of PLGA was selected because it has not been published nor documented and is of personal interest to the authors. Additionally, PLGA is expensive and so conducting experimental research with it requires significant funding. This work suggests that LLMs could be used to predict the outcomes of using expensive materials in research, and the results could be used to select which materials are used for real studies. In hindsight, PLGA was an ideal polymer for this study due to the copious amount of information available on its use and because of its applications in many material and healthcare sectors (Wang et al., 2022a). This is in contrast to some pharmaceutical polymers for which there are a lack of published data because they are almost exclusively used in pharmaceutical research and their chemical structures have not been disclosed by their manufacturers. It would be interesting to see how AI would simulate data based on these materials.

Data remains the main issue in using AI in pharmaceutics. All AI systems look to published data to draw relationships between chemical structure, physicochemical properties and behaviour in formulated medicines. Without open source data an AI system cannot develop relationships which it can use to predict outcomes. On the other hand, because the use of AI to generate scientific data is a new paradigm, most of the data in the literature have been generated by experimental research and any relationships between materials is real. If AI-generated data begin to populate the internet, then there will be an increasing proportion of data that are not real, and there is a risk that AI models start to predict non-sensical outcomes (this is already an issue being seen in the field of art, for instance). It may be the case that technologies such as blockchain can circumvent this issue (Trenfield et al., 2022), but the authors strongly suggest that all published data generated with AI are

marked as such, so that they are not incorporated into future predictions by AI models. We also note that regulations will indeed be needed. For one, models should be closely monitored to ensure that they are trained with high quality, unbiased data, and they should be robust to adversarial attacks (Chen et al., 2023; Kaviani et al., 2022). There has been concern regarding LLMs 'hallucinating' responses, whereby they generate fictitious information (Brodnik et al., 2023). However, this is being actively addressed and once achieved, it is anticipated that it will result in more accurate experimental simulations.

The ability of LLMs to generate different data of multiple types clearly demonstrates multi-disciplinary expertise beyond the pharmaceutical sciences. Future work will seek to stretch its use to new data modalities and to evaluate the extent of its multi-disciplinary expertise. In addition, while communicating with AI via human languages makes it more widely accessible than communicating with it via coding, it will be interesting to see if it can be made even more accessible, for example by ensuring any AI platform will be economically viable and not hidden behind a paywall (Liebrenz et al., 2023).

4. Conclusion

We have demonstrated how GPT-4, an LLM, can simulate completion of a research project on a topic that is itself novel. It was able to conceive a research hypothesis, define an experimental protocol, produce photo-realistic images of the printlets, generate believable analytical data from a range of instruments and write a convincing publication-ready manuscript with evidence of critical interpretation. The model achieved all this is less than 1h. While caution must be exercised in the value placed on the research outcomes, we have nonetheless shown the potential power of AI in accelerating research. If the data generated this way are representative of reality, then AI could be used to save time and cost as well as limit the environmental impact of research.

5. Acknowledgements

Moe Elbadawi thanks EPSRC for funding (EP/S009000/1)

References

Abdalla, Y., Elbadawi, M., Ji, M., Alkahtani, M., Awad, A., Orlu, M., Gaisford, S., Basit, A.W., 2023. Machine learning using multi-modal data predicts the production

of selective laser sintered 3D printed drug products. International Journal of Pharmaceutics 633, 122628.

Agathokleous, E., Rillig, M.C., Peñuelas, J., Yu, Z., 2023. One hundred important questions facing plant science derived using a large language model. Trends in Plant Science.

Awad, A., Fina, F., Trenfield, S.J., Patel, P., Goyanes, A., Gaisford, S., Basit, A.W., 2019. 3D Printed Pellets (Miniprintlets): A Novel, Multi-Drug, Controlled Release Platform Technology. Pharmaceutics 11, 148.

Bannigan, P., Bao, Z., Hickman, R.J., Aldeghi, M., Häse, F., Aspuru-Guzik, A., Allen, C., 2023. Machine learning models to accelerate the design of polymeric long-acting injectables. Nature Communications 14, 35.

Briganti, G., Le Moine, O., 2020. Artificial Intelligence in Medicine: Today and Tomorrow. Frontiers in Medicine 7.

Brodnik, N.R., Carton, S., Muir, C., Ghosh, S., Downey, D., Echlin, M.P., Pollock, T.M., Daly, S., 2023. Perspective: Large Language Models in Applied Mechanics. Journal of Applied Mechanics 90.

Charoo, N.A., Barakh Ali, S.F., Mohamed, E.M., Kuttolamadom, M.A., Ozkan, T., Khan, M.A., Rahman, Z., 2020. Selective laser sintering 3D printing – an overview of the technology and pharmaceutical applications. Drug Development and Industrial Pharmacy 46, 869-877.

Chen, H., Engkvist, O., Wang, Y., Olivecrona, M., Blaschke, T., 2018. The rise of deep learning in drug discovery. Drug Discovery Today 23, 1241-1250.

Chen, R.J., Wang, J.J., Williamson, D.F.K., Chen, T.Y., Lipkova, J., Lu, M.Y., Sahai, S., Mahmood, F., 2023. Algorithmic fairness in artificial intelligence for medicine and healthcare. Nature Biomedical Engineering 7, 719-742.

Das, P., Sercu, T., Wadhawan, K., Padhi, I., Gehrmann, S., Cipcigan, F., Chenthamarakshan, V., Strobelt, H., dos Santos, C., Chen, P.-Y., Yang, Y.Y., Tan, J.P.K., Hedrick, J., Crain, J., Mojsilovic, A., 2021. Accelerated antimicrobial discovery via deep generative models and molecular dynamics simulations. Nature Biomedical Engineering 5, 613-623.

Davis, D.A., Miller, D.A., Su, Y., Williams, R.O., 2020. Thermally Conductive Excipient Expands KinetiSol® Processing Capabilities. AAPS PharmSciTech 21, 319.

De Angelis, L., Baglivo, F., Arzilli, G., Privitera, G.P., Ferragina, P., Tozzi, A.E., Rizzo, C., 2023. ChatGPT and the rise of large language models: the new AI-driven infodemic threat in public health. Frontiers in Public Health 11.

de Oliveira, G.G.G., Feitosa, A., Loureiro, K., Fernandes, A.R., Souto, E.B., Severino, P., 2017. Compatibility study of paracetamol, chlorpheniramine maleate and phenylephrine hydrochloride in physical mixtures. Saudi Pharmaceutical Journal 25, 99-103.

Dedeloudi, A., Weaver, E., Lamprou, D.A., 2023. Machine learning in additive manufacturing & Microfluidics for smarter and safer drug delivery systems. International Journal of Pharmaceutics 636, 122818.

Dou, Y., Huang, J., Xia, X., Wei, J., Zou, Q., Zuo, Y., Li, J., Li, Y., 2021. A hierarchical scaffold with a highly pore-interconnective 3D printed PLGA/n-HA framework and an extracellular matrix like gelatin network filler for bone regeneration. Journal of Materials Chemistry B 9, 4488-4501.

Elbadawi, M., Basit, A.W., Gaisford, S., 2023. Energy consumption and carbon footprint of 3D printing in pharmaceutical manufacture. International Journal of Pharmaceutics 639, 122926.

Elbadawi, M., McCoubrey, L.E., Gavins, F.K.H., Ong, J.J., Goyanes, A., Gaisford, S., Basit, A.W., 2021. Disrupting 3D printing of medicines with machine learning. Trends in Pharmacological Sciences 42, 745-757.

Elbadawi, M., Muñiz Castro, B., Gavins, F.K.H., Ong, J.J., Gaisford, S., Pérez, G., Basit, A.W., Cabalar, P., Goyanes, A., 2020. M3DISEEN: A novel machine learning approach for predicting the 3D printability of medicines. International Journal of Pharmaceutics 590, 119837.

Elbadawi, M., Li, H., Basit, A., Gaisford, S. 2024. Artificial Intelligence generates novel 3D printing formulations. Advanced Pharmaceutical Materials, *submitted.*

Englezos, K., Wang, L., Tan, E.C.K., Kang, L., 2023. 3D printing for personalised medicines: implications for policy and practice. International Journal of Pharmaceutics 635, 122785.

Ficzere, M., Mészáros, L.A., Kállai-Szabó, N., Kovács, A., Antal, I., Nagy, Z.K., Galata, D.L., 2022. Real-time coating thickness measurement and defect recognition of film coated tablets with machine vision and deep learning. International Journal of Pharmaceutics 623, 121957.

Fina, F., Goyanes, A., Gaisford, S., Basit, A.W., 2017. Selective laser sintering (SLS) 3D printing of medicines. International Journal of Pharmaceutics 529, 285-293.

Floridi, L., Chiriatti, M., 2020. GPT-3: Its Nature, Scope, Limits, and Consequences. Minds and Machines 30, 681-694.

Frye, B.L., 2022. Should using an AI text generator to produce academic writing be plagiarism? Fordham Intellectual Property, Media & Entertainment Law Journal, Forthcoming.

Galata, D.L., Mészáros, L.A., Kállai-Szabó, N., Szabó, E., Pataki, H., Marosi, G., Nagy, Z.K., 2021. Applications of machine vision in pharmaceutical technology: A review. European Journal of Pharmaceutical Sciences 159, 105717.

Gao, A., Murphy, R.R., Chen, W., Dagnino, G., Fischer, P., Gutierrez, M.G., Kundrat, D., Nelson, B.J., Shamsudhin, N., Su, H., Xia, J., Zemmar, A., Zhang, D., Wang, C., Yang, G.-Z., 2021. Progress in robotics for combating infectious diseases. Science Robotics 6, eabf1462.

Gavins, F.K.H., Fu, Z., Elbadawi, M., Basit, A.W., Rodrigues, M.R.D., Orlu, M., 2022. Machine learning predicts the effect of food on orally administered medicines. International Journal of Pharmaceutics 611, 121329.

Giri, B.R., Maniruzzaman, M., 2022. Fabrication of Sustained-Release Dosages Using Powder-Based Three-Dimensional (3D) Printing Technology. AAPS PharmSciTech 24, 4.

Goyanes, A., Robles Martinez, P., Buanz, A., Basit, A.W., Gaisford, S., 2015. Effect of geometry on drug release from 3D printed tablets. International Journal of Pharmaceutics 494, 657-663.

Holler, J., Levinson, S.C., 2019. Multimodal Language Processing in Human Communication. Trends in Cognitive Sciences 23, 639-652.

Jeong, J., Yoon, S., Yang, X., Kim, Y.J., 2023. Super-Tough and Biodegradable Poly(lactide-co-glycolide) (PLGA) Transparent Thin Films Toughened by Star-Shaped PCL-b-PDLA Plasticizers. Polymers 15, 2617.

Jose, M.V., Thomas, V., Dean, D.R., Nyairo, E., 2009. Fabrication and characterization of aligned nanofibrous PLGA/Collagen blends as bone tissue scaffolds. Polymer 50, 3778-3785.

Kaviani, S., Han, K.J., Sohn, I., 2022. Adversarial attacks and defenses on AI in medical imaging informatics: A survey. Expert Systems with Applications 198, 116815.

Khaled, S.A., Alexander, M.R., Irvine, D.J., Wildman, R.D., Wallace, M.J., Sharpe, S., Yoo, J., Roberts, C.J., 2018a. Extrusion 3D Printing of Paracetamol Tablets from a Single Formulation with Tunable Release Profiles Through Control of Tablet Geometry. AAPS PharmSciTech 19, 3403-3413.

Khaled, S.A., Alexander, M.R., Wildman, R.D., Wallace, M.J., Sharpe, S., Yoo, J., Roberts, C.J., 2018b. 3D extrusion printing of high drug loading immediate release paracetamol tablets. International Journal of Pharmaceutics 538, 223-230.

Kim, S., Choi, Y., Won, J.-H., Mi Oh, J., Lee, H., 2022. An annotated corpus from biomedical articles to construct a drug-food interaction database. Journal of Biomedical Informatics 126, 103985.

Kung, T.H., Cheatham, M., Medenilla, A., Sillos, C., De Leon, L., Elepaño, C., Madriaga, M., Aggabao, R., Diaz-Candido, G., Maningo, J., Tseng, V., 2023. Performance of ChatGPT on USMLE: Potential for AI-assisted medical education using large language models. PLOS Digital Health 2, e0000198.

Lanao, R.P.F., Jonker, A.M., Wolke, J.G., Jansen, J.A., van Hest, J.C., Leeuwenburgh, S.C., 2013. Physicochemical properties and applications of poly (lactic-co-glycolic acid) for use in bone regeneration. Tissue Engineering Part B: Reviews 19, 380-390.

Liebrenz, M., Schleifer, R., Buadze, A., Bhugra, D., Smith, A., 2023. Generating scholarly content with ChatGPT: ethical challenges for medical publishing. The Lancet Digital Health 5, e105-e106.

Madžarević, M., Medarević, Đ., Pavlović, S., Ivković, B., Đuriš, J., Ibrić, S., 2021. Understanding the Effect of Energy Density and Formulation Factors on the Printability and Characteristics of SLS Irbesartan Tablets—Application of the Decision Tree Model. Pharmaceutics 13, 1969.

Marquez, R., Barrios, N., Vera, R.E., Mendez, M.E., Tolosa, L., Zambrano, F., Li, Y., 2023. A perspective on the synergistic potential of artificial intelligence and product-based learning strategies in biobased materials education. Education for Chemical Engineers 44, 164-180.

McCoubrey, L.E., Seegobin, N., Elbadawi, M., Hu, Y., Orlu, M., Gaisford, S., Basit, A.W., 2022. Active Machine learning for formulation of precision probiotics. International Journal of Pharmaceutics 616, 121568.

Norris, C., 2023. Large Language Models Like ChatGPT in ABME: Author Guidelines. Annals of Biomedical Engineering 51, 1121-1122.

O'Reilly, C.S., Elbadawi, M., Desai, N., Gaisford, S., Basit, A.W., Orlu, M., 2021. Machine Learning and Machine Vision Accelerate 3D Printed Orodispersible Film Development. Pharmaceutics 13, 2187.

Olvera, D., Monaghan, M.G., 2021. Electroactive material-based biosensors for detection and drug delivery. Advanced Drug Delivery Reviews 170, 396-424.

Palagi, S., Fischer, P., 2018. Bioinspired microrobots. Nature Reviews Materials 3, 113-124.

Popova, M., Isayev, O., Tropsha, A., 2018. Deep reinforcement learning for de novo drug design. Science Advances 4, eaap7885.

Prasad, E., Islam, M.T., Goodwin, D.J., Megarry, A.J., Halbert, G.W., Florence, A.J., Robertson, J., 2019. Development of a hot-melt extrusion (HME) process to produce drug loaded Affinisol™ 15LV filaments for fused filament fabrication (FFF) 3D printing. Additive Manufacturing 29, 100776.

Rahimi, F., Talebi Bezmin Abadi, A., 2023. ChatGPT and Publication Ethics. Archives of Medical Research 54, 272-274.

Raijada, D., Wac, K., Greisen, E., Rantanen, J., Genina, N., 2021. Integration of personalized drug delivery systems into digital health. Advanced Drug Delivery Reviews, 113857.

Rodrigues, C.P., Duchesne, C., Poulin, É., Lapointe-Garant, P.-P., 2021. In-line cosmetic end-point detection of batch coating processes for colored tablets using multivariate image analysis. International Journal of Pharmaceutics 606, 120953.

Shi, Y., xue, J., Jia, L., Du, Q., Niu, J., Zhang, D., 2018. Surface-modified PLGA nanoparticles with chitosan for oral delivery of tolbutamide. Colloids and Surfaces B: Biointerfaces 161, 67-72.

Thirunavukarasu, A.J., Ting, D.S.J., Elangovan, K., Gutierrez, L., Tan, T.F., Ting, D.S.W., 2023. Large language models in medicine. Nature Medicine.

Trenfield, S.J., Awad, A., McCoubrey, L.E., Elbadawi, M., Goyanes, A., Gaisford, S., Basit, A.W., 2022. Advancing pharmacy and healthcare with virtual digital technologies. Advanced Drug Delivery Reviews 182, 114098.

Trewartha, A., Walker, N., Huo, H., Lee, S., Cruse, K., Dagdelen, J., Dunn, A., Persson, K.A., Ceder, G., Jain, A., 2022. Quantifying the advantage of domain-specific pre-training on named entity recognition tasks in materials science. Patterns 3, 100488.

von Erlach, T., Saxton, S., Shi, Y., Minahan, D., Reker, D., Javid, F., Lee, Y.-A.L., Schoellhammer, C., Esfandiary, T., Cleveland, C., Booth, L., Lin, J., Levy, H., Blackburn, S., Hayward, A., Langer, R., Traverso, G., 2020. Robotically handled whole-tissue culture system for the screening of oral drug formulations. Nature Biomedical Engineering 4, 544-559.

Walejewska, E., Idaszek, J., Heljak, M., Chlanda, A., Choinska, E., Hasirci, V., Swieszkowski, W., 2020. The effect of introduction of filament shift on degradation behaviour of PLGA- and PLCL-based scaffolds fabricated via additive manufacturing. Polymer Degradation and Stability 171, 109030.

Wang, F., Elbadawi, M., Tsilova, S.L., Gaisford, S., Basit, A.W., Parhizkar, M., 2022a. Machine learning predicts electrospray particle size. Materials & Design 219, 110735.

Wang, F., Elbadawi, M., Tsilova, S.L., Gaisford, S., Basit, A.W., Parhizkar, M., 2022b. Machine learning to empower electrohydrodynamic processing. Materials Science and Engineering: C 132, 112553.

Wang, F., Sangfuang, N., McCoubrey, L.E., Yadav, V., Elbadawi, M., Orlu, M., Gaisford, S., Basit, A.W., 2023a. Advancing oral delivery of biologics: Machine learning predicts peptide stability in the gastrointestinal tract. International Journal of Pharmaceutics 634, 122643.

Wang, H., Fu, T., Du, Y., Gao, W., Huang, K., Liu, Z., Chandak, P., Liu, S., Van Katwyk, P., Deac, A., Anandkumar, A., Bergen, K., Gomes, C.P., Ho, S., Kohli, P., Lasenby, J., Leskovec, J., Liu, T.-Y., Manrai, A., Marks, D., Ramsundar, B., Song, L., Sun, J., Tang, J., Veličković, P., Welling, M., Zhang, L., Coley, C.W., Bengio, Y., Zitnik, M., 2023b. Scientific discovery in the age of artificial intelligence. Nature 620, 47-60.

Wei, J., Yan, Y., Gao, J., Li, Y., Wang, R., Wang, J., Zou, Q., Zuo, Y., Zhu, M., Li, J., 2022. 3D-printed hydroxyapatite microspheres reinforced PLGA scaffolds for bone regeneration. Biomaterials Advances 133, 112618.

Xu, Y., Liu, X., Cao, X., Huang, C., Liu, E., Qian, S., Liu, X., Wu, Y., Dong, F., Qiu, C.-W., Qiu, J., Hua, K., Su, W., Wu, J., Xu, H., Han, Y., Fu, C., Yin, Z., Liu, M., Roepman, R., Dietmann, S., Virta, M., Kengara, F., Zhang, Z., Zhang, L., Zhao, T., Dai, J., Yang, J., Lan, L., Luo, M., Liu, Z., An, T., Zhang, B., He, X., Cong, S., Liu, X., Zhang, W., Lewis, J.P., Tiedje, J.M., Wang, Q., An, Z., Wang, F., Zhang, L., Huang, T., Lu, C., Cai, Z., Wang, F., Zhang, J., 2021. Artificial intelligence: A powerful paradigm for scientific research. The Innovation 2, 100179.

Zhang, Y., Thakkar, R., Zhang, J., Lu, A., Duggal, I., Pillai, A., Wang, J., Aghda, N.H., Maniruzzaman, M., 2023. Investigating the Use of Magnetic Nanoparticles As Alternative Sintering Agents in Selective Laser Sintering (SLS) 3D Printing of Oral Tablets. ACS Biomaterials Science & Engineering 9, 2924-2936.

Appendix: AI-generated manuscript

Fabrication of Drug-Loaded PLGA via Selective Laser Sintering (SLS)

Abstract

Poly(lactic-co-glycolic acid) (PLGA) stands out in the pharmaceutical sector, given its tunable degradation rates, FDA approval, and adaptability for both medicines and medical devices. Despite these promising attributes, PLGA's potential when combined with Selective Laser Sintering (SLS), a cutting-edge 3D printing technology, remains untapped. SLS offers precision layering and adaptability to various polymeric materials, making it an ideal candidate for realizing the full potential of PLGA in drug delivery systems. This study pioneers the application of SLS in fabricating PLGA printlets embedded with paracetamol. Comprehensive characterization verified the successful integration of paracetamol into the PLGA matrix. Thermal evaluations via TGA and DSC underscored the printlets' exceptional thermal stability, crucial for uniform drug release. Mechanical tests delineated the influence of sintering dynamics, revealing that laser speed adjustments produce robust printlets fit for physiological conditions. Further, dissolution studies depicted a controlled, prolonged release of paracetamol, emphasizing its potential in chronotherapy. This investigation not only showcases the unmatched versatility of PLGA in tandem with SLS but also posits a transformative trajectory in pharmaceutical manufacturing, emphasizing the significance of harnessing such synergies for futuristic, patient-centric drug delivery solutions.

Introduction

The integration of 3D printing technologies into the pharmaceutical landscape has heralded a paradigm shift in drug formulation and delivery systems. Emerging from the broader sphere of additive manufacturing, 3D printed medicines offer the unparalleled ability to craft patient-specific dosages, geometries, and release profiles, potentially revolutionizing personalized healthcare approaches. In this continuously evolving landscape, it's imperative to explore and understand the most compatible materials that lend themselves to these novel manufacturing techniques.

Poly(lactic-co-glycolic acid) (PLGA) is a biodegradable and biocompatible polymer extensively researched for its promising attributes in drug delivery applications. Its inherent properties, such as tunable degradation rates and the ability to encapsulate a wide range of therapeutic agents, make it an ideal candidate for incorporation into 3D printed pharmaceutical structures. Furthermore, PLGA's safety profile, already validated through various FDA-approved products, underscores its significance in translational medicine.

However, the interplay between PLGA and various 3D printing techniques remains an area warranting further investigation. Selective laser sintering (SLS) is one such technique that offers distinct advantages, including high resolution and the ability to produce complex geometries without the need for support structures. Yet, despite its potential, studies that delve into the intricacies of drug-loaded PLGA structures fabricated by SLS are limited.

Recognizing this research lacuna, our study embarks on a detailed exploration of the capabilities and intricacies of SLS in fabricating drug-loaded PLGA structures. Through this endeavor, we aim to elucidate the potential synergies and challenges, offering insights that could pave the way for groundbreaking innovations in the realm of drug delivery systems.

Experimental Procedure

Raw Material Acquisition: PLGA was sourced from Evonik Industries AG (Darmstadt, Germany) with an inherent viscosity of 0.55–0.75 dL/g. Paracetamol (acetaminophen) was obtained from Sigma-Aldrich (St. Louis, MO, USA). Candurin gold sheen was procured from Merck KGaA (Darmstadt, Germany). For the dissolution study, a carefully prepared phosphate buffer solution (pH 6.8) was used. This medium was composed of monosodium phosphate (NaH_2PO_4) sourced from Fisher Scientific, which acted as the primary buffering agent, and disodium phosphate (Na_2HPO_4) procured from Merck KGaA, both ensuring a stable pH throughout the dissolution process. Necessary pH adjustments to achieve the exact 6.8 value were performed using sodium hydroxide (NaOH) from Sigma-Aldrich and hydrochloric acid (HCl) from VWR. The entire solution was prepared using high-quality distilled water, obtained from Honeywell, ensuring the absence of impurities that might interfere with the dissolution results.

Powder Preparation: PLGA was cryo-milled at -196°C using liquid nitrogen to produce fine particles. Milling was conducted for 3 hours to ensure homogeneity. Paracetamol and candurin gold sheen were separately milled using the same procedure. The milled powders were then carefully weighed in desired ratios and mixed together using a mechanical blender for 1 hour to ensure a uniform distribution.

SLS Printing: The tablet design was conceptualized using Computer-Aided Design (CAD) software, SolidWorks (Dassault Systèmes, France). Precise dimensions, geometries, and specifications were set according to the required drug dosage and desired release profile. The finalized design was saved in STL (stereolithography) format, optimized for the SLS printing process. The composite powder, consisting of

PLGA, paracetamol, and candurin gold sheen, was carefully loaded into the Sintratec Kit — an SLS 3D printer known for its compatibility with a range of polymers and equipped with a blue diode laser. The printer's settings were meticulously calibrated to cater to the specific properties of the mixed materials, ensuring optimal sintering conditions. The parameters can be found in Table 1. The CAD tablet design, saved in STL format, was imported into the Sintratec Central software. The printing commenced, layer-by-layer, with the blue diode laser selectively sintering the material according to the design's specifications. Post printing, the chamber was left undisturbed, allowing for a uniform cool-down to room temperature over 12 hours. This procedure is crucial to ascertain material stability and retain the tablet's structural integrity. After adequate cooling, the 3D printed tablets were delicately removed from the print bed, ensuring no damage or deformation during extraction.

Table 3 *SLS parameters*

Parameter	**Value**
Laser Type	Blue Diode
Laser Power	-
Scan Speed	100-500 mm/s
Layer Thickness	100 µm
Hatch distance	0.25 mm
Print Bed Temperature	The print bed temperature was modulated, holding it slightly below the PLGA's glass transition temperature to inhibit pre-mature sintering.

Characterization:

Differential Scanning Calorimetry (DSC)

Samples were accurately weighed (~5 mg) and sealed in aluminium pans. Thermal analysis was conducted from 25°C to 300°C at a heating rate of 10°C/min using a DSC 200 F3 Maia (NETZSCH, Germany).

Thermogravimetric Analysis (TGA)

Approximately 10 mg of the sample was heated from 25°C to 600°C at 10°C/min under a nitrogen atmosphere using TGA 209 F1 Iris (NETZSCH, Germany).

X-ray Diffraction (XRD)

XRD patterns were recorded using a D8 Advance diffractometer (Bruker, Germany). Scanning was done from 5° to 50° (2θ) at a rate of 2°/min.

Fourier Transform Infrared Spectroscopy (FTIR)

FTIR spectra were acquired on a Nicolet iS50 FTIR Spectrometer (Thermo Fisher Scientific). The KBr pellet method was used, and spectra were recorded between 4000 and 400 cm^{-1}.

X-ray Micro Computed Tomography (Micro CT)

The micro-computed tomography (micro-CT) examinations were conducted using the SkyScan 1272 system (Bruker, Belgium). The instrument was configured with an X-ray source set at a tube voltage of 60 kV and a current of 166 µA. A 0.5 mm aluminum filter was strategically positioned to enhance image contrast by filtering out lower energy photons. For each session, samples were meticulously mounted onto the sample holder to ascertain stability and prevent any movements during the scanning process. Care was taken to center the region of interest within the scanner's field of view. The scanning regimen was set to encompass a full 360° rotation of the sample with intermediate rotation steps set at 0.4° between consecutive X-ray projections. To bolster the signal-to-noise ratio, an average of 3 frames was taken for each projection. The exposure time was finely adjusted, ranging between 500 to 1000 ms, depending on the sample's intrinsic density and size. Post-acquisition, the raw projection data were promptly fed into the NRecon software (Bruker, Belgium) for the reconstruction phase. Initial steps involved aligning the projections to ensure the reconstructed images' fidelity. Ring artifact correction was initiated and set to a level of 10, aiming to diminish the typical ring artifacts inherent in micro-CT outputs. Furthermore, to counteract the beam hardening effects, a correction value was set at 30%. Subsequent to the reconstruction, the output data were visualized as both 2D slices and comprehensive 3D volume renderings. Following reconstruction, the data underwent a quantitative

assessment using the CTAn software suite (Bruker). This stage was pivotal for extracting critical parameters, such as porosity, distribution of pore sizes, and the structural thickness inherent in the samples. To ensure data integrity and future accessibility, both raw and processed datasets were systematically stored on dedicated storage systems.

Drug Dissolution

The objective of the drug dissolution study was to assess the release rate of paracetamol from the SLS-fabricated PLGA tablets under simulated physiological conditions. The process was executed as per standardized protocols, ensuring the replicability and reliability of the results. The dissolution apparatus used for this study was a USP Type II (paddle method) system. This system is commonly used for dosage forms that exhibit a tendency to float, ensuring a uniform agitation to derive accurate dissolution profiles.

The vessel of the apparatus was filled with a pre-defined volume of dissolution medium, maintaining a pH of 6.8, which closely simulates the pH of the small intestine, providing insights into the potential in vivo drug release patterns. The temperature of the dissolution medium was stringently maintained at 37°C throughout the experiment, mimicking human body temperature.

Tablets were carefully placed in the dissolution vessels, ensuring they were fully immersed in the medium. The paddle speed was set at 100 rpm, a commonly used speed that ensures a consistent and gentle agitation of the medium without causing any disintegration of the tablet. Throughout the dissolution process, samples were recorded on a daily basis. Using a pipette, aliquots were precisely taken from the medium at specific intervals, ensuring minimal disturbance to the remaining medium and the tablet. Once the aliquots were extracted, they were immediately subjected to analysis to determine the concentration of paracetamol. A UV-visible spectrophotometer was employed for this purpose. The aliquots were placed in cuvettes, and the absorbance was measured at a 243 nm. This ensured that only the paracetamol's concentration was detected, eliminating interference from other constituents. Calibration curves were previously prepared using known concentrations of paracetamol, which provided a reference for determining the concentrations in the aliquots. Results from the spectrophotometer were tabulated and plotted to establish the dissolution profile of paracetamol from the PLGA tablets over time. The meticulous recording and detailed analysis enabled a comprehensive understanding of the drug release behavior of the SLS-fabricated PLGA tablets, providing invaluable insights for potential therapeutic applications.

Data Analysis

Data derived from each characterization technique was comprehensively analyzed using the respective software packages, ensuring all peaks, troughs, and anomalies were documented and interpreted. Figure 1 presents the methodology pipeline.

Figure 1. *Schematic of the Methodology pipeline*

Results

Utilizing the detailed CAD model as shown in Figure 2 (A), PLGA loaded with paracetamol was effectively sintered, yielding printlets with consistent and expected morphologies. The CAD model served as a pivotal guide, ensuring accurate alignment and distribution of PLGA tablets during the sintering process. This successful realization is visually captured in Figure 2 (B), where the images display the printlets that resulted from the process, underscoring the precision of the method and the uniformity of the drug distribution within the PLGA framework.

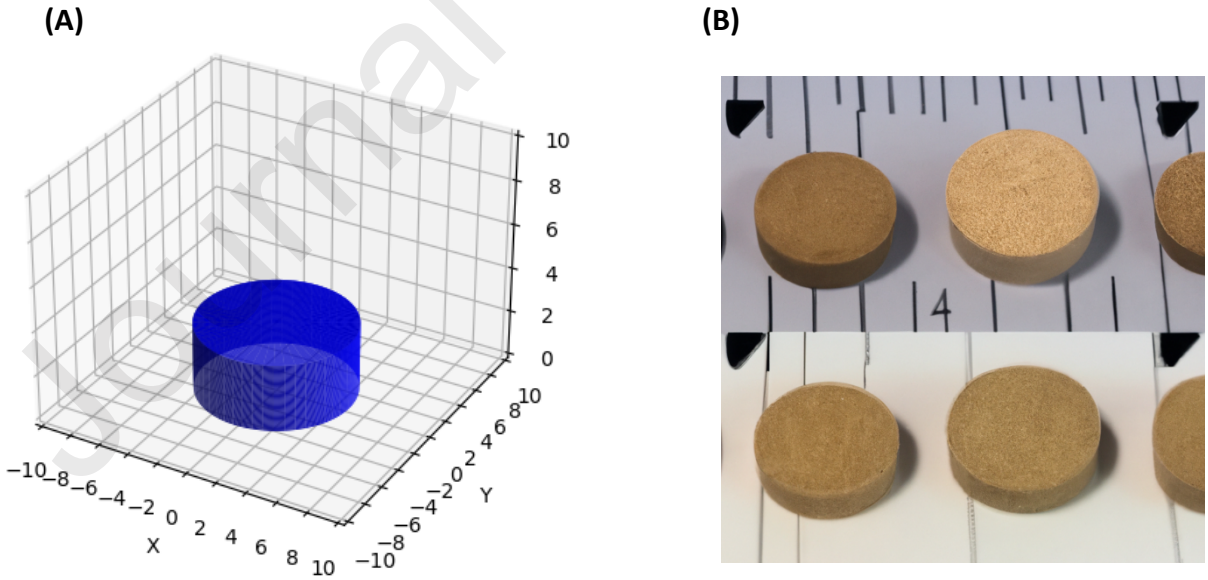

Figure 2. (A) *CAD of 10 x 3 mm tablet and* ***(B)*** *images of the SLS-printed PLGA*

Thermal Analyses

Thermogravimetric Analysis (TGA) was employed to investigate the thermal degradation profiles of PLGA, Paracetamol, and Candurin, alongside a composite feedstock comprising these components (Figure 3 (A)). From the range of 25°C to 600°C, the weight percent remaining versus temperature exhibited distinct decomposition characteristics for each substance. PLGA displayed an initial decomposition stage between 60°C and 90°C, with the weight loss apex at approximately 70°C, shedding around 10% of its weight. A more significant decomposition was noted between 280°C and 320°C, where the substance underwent an 88% weight loss, with the steepest drop around 300°C. In contrast, Paracetamol's thermal degradation began between 140°C and 170°C, centering at 150°C with a 5% weight decrease. The primary decomposition stage for Paracetamol manifested between 230°C and 270°C, during which it lost up to 95% of its weight, peaking at 250°C. Candurin, on the other hand, started its degradation at a higher temperature bracket of 470°C to 500°C, registering a 5% weight loss at 480°C. Its subsequent weight reduction was identified between 560°C and 600°C, amounting to a 10% loss and peaking at 580°C. Of particular interest was the thermal profile of the composite feedstock, formulated with 87% PLGA, 10% Paracetamol, and 3% Candurin. Its decomposition trend, illustrated by a distinct dashed curve in the graph, encapsulated the thermal behaviors of its individual constituents. This combined thermal profile of the feedstock provided insights into its composite behavior during elevated temperatures, hinting at the complexities arising from the interaction of its individual components. In summary, the TGA analysis delineated the individual and combined thermal degradation patterns of PLGA, Paracetamol, and Candurin. Such insights are crucial for understanding material stability under varying temperature conditions, especially in applications where thermal performance is paramount.

Differential Scanning Calorimetry (DSC) was employed to study the thermal transitions of PLGA, Paracetamol, and Candurin, along with a composite feedstock of these materials and a sample from Selective Laser Sintering (SLS) printing (Figure 3(B)). The thermal spectra were recorded over a temperature range from 0°C to 200°C and depicted the heat flow in normalized units. For PLGA, two notable transitions were identified. A glass transition (Tg) occurred at approximately 50°C, reflected by a minor endothermic peak. This was closely followed by a sharper melting peak (Tm) centered around 60°C. Paracetamol displayed a prominent melting transition, as indicated by a pronounced endothermic peak at about 170°C. On the other hand, within the tested temperature bracket, Candurin did not manifest any discernible thermal transitions. The composite feedstock spectrum, derived from an 87% contribution of PLGA, 10% from Paracetamol, and 3% from Candurin, portrayed an overlapping spectrum inheriting transitions from its components. It is noteworthy that the SLS-printed sample exhibited a distinct spectrum from the feedstock. Within this SLS sample, the Paracetamol appeared amorphous, as evidenced by the absence of its characteristic melting peak. The graphical representation offers a comprehensive visualization of the thermal events. The plots for raw PLGA, Paracetamol, and Candurin are presented with ascending offsets for clarity. The feedstock and SLS-printed spectra are also plotted with incremental

offsets, allowing for clear distinction and comparison between each sample. The use of Differential Scanning Calorimetry in this context provides invaluable insights into the thermal behaviors of these materials, particularly when combined or subjected to manufacturing techniques such as SLS.

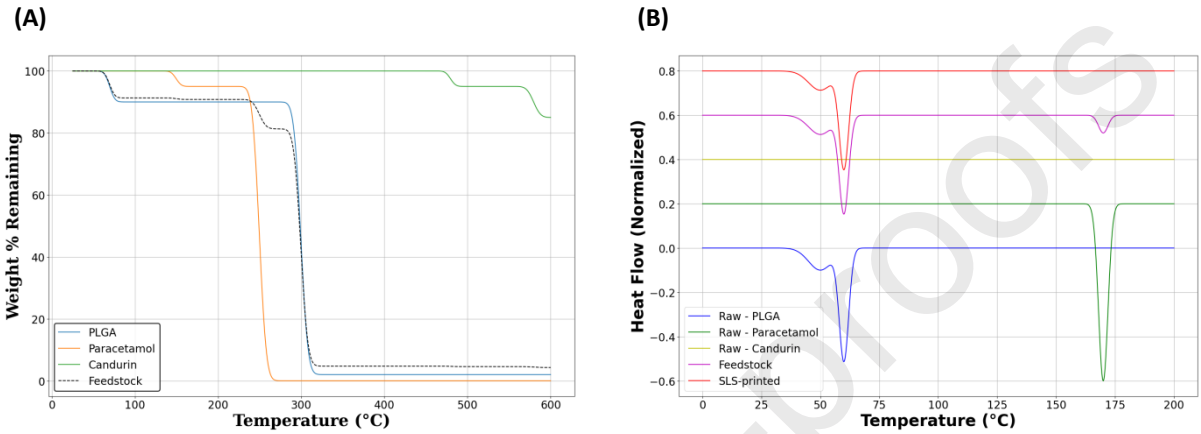

Figure 3 (A) *TGA and* ***(B)*** *DSC thermograms of results.*

Chemical Structure

Fourier-Transform Infrared Spectroscopy (FTIR) was employed to investigate the vibrational spectra of three materials: PLGA, Paracetamol, and Candurin. These spectra offer insights into the molecular compositions and structures of the materials.

In the spectrum of PLGA, distinct peaks were evident at various wavenumbers (Figure 4 (A)). The peaks at around 2950 cm^{-1} and 2850 cm^{-1} correspond to C-H stretching of methine and methylene groups, respectively. A robust and sharp peak around 1750 cm^{-1} is indicative of C=O stretching, while those around 1450 cm^{-1} and 1380 cm^{-1} are attributed to C-H bending. Furthermore, several peaks ranging from 1300 cm^{-1} to 1050 cm^{-1} are evident, suggesting multiple functional groups or vibrational modes within this range. Paracetamol's spectrum, on the other hand, exhibited a broad peak around 3300 cm^{-1}, indicating O-H stretching. The amide functionalities in Paracetamol resulted in distinct peaks. Specifically, Amide I and Amide II were marked by peaks at approximately 1650 cm^{-1} (C=O stretching) and 1550 cm^{-1} (N-H bending) respectively, while Amide III, corresponding to C-N stretching, was observed at around 1300 cm^{-1}. The aromatic ring vibrations and bending modes in Paracetamol are discernible from the plethora of peaks spanning from 1600 cm^{-1} to 650 cm^{-1}. Candurin presented a peak around 3500 cm^{-1}, signifying O-H stretching possibly from mica. The peak at approximately 1050 cm^{-1} is attributed to Si-O-Si stretching, also from mica. Peaks around 600 cm^{-1} and 500 cm^{-1} can be associated with Fe-O and Ti-O stretching respectively, possibly hinting

at the presence of iron oxide and titanium dioxide in Candurin. The feedstock's spectrum is a composite, predominantly influenced by PLGA (87% contribution), followed by Paracetamol (10%) and a minor contribution from Candurin (3%). Of note is the spectrum of an SLS-printed material, where Paracetamol appears amorphous, evidenced by broader and less intense peaks compared to its crystalline counterpart. The FTIR spectra, with their distinct peaks and profiles, offer invaluable insights into the molecular structures and interactions of the materials, particularly when these materials undergo processes that might influence their structural integrities, such as SLS printing.

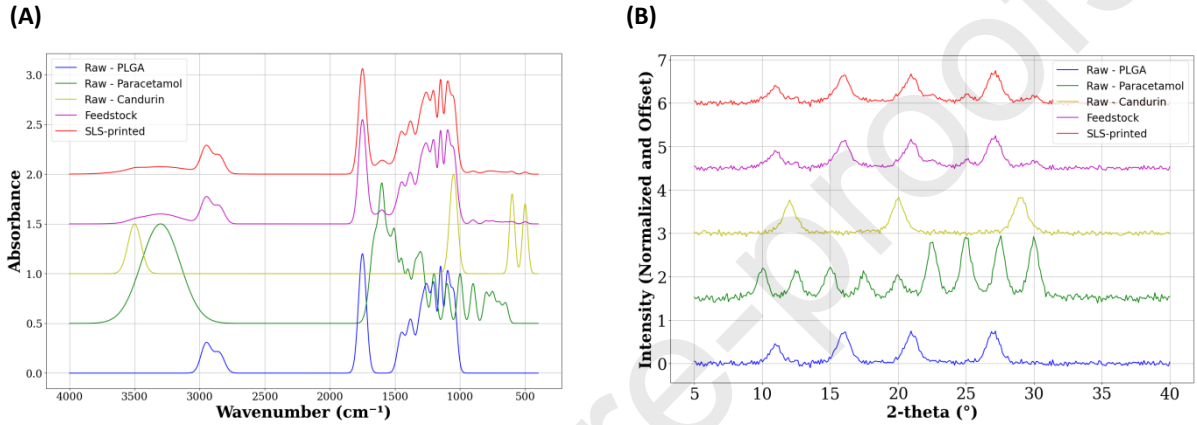

Figure 4 (A) *FTIR and* ***(B)*** *XRD results.*

X-ray diffraction (XRD) patterns provided critical insight into the crystalline structures of PLGA, Paracetamol, Candurin, and their respective mixtures (Figure 4 (B)). Each material showcased its own characteristic diffraction pattern within the 2-theta range of 5° to 40°. The raw PLGA sample presented clear and distinct peaks, with pronounced reflections observed around the 2-theta values of 11°, 16°, 21°, and 27°. These peaks affirm its semi-crystalline nature, and the sharpness of these reflections alludes to a well-ordered crystalline arrangement within the material. For the raw Paracetamol sample, a series of peaks spanning the 10° to 30° range were visible. The multiplicity of these peaks suggests a relatively complex crystalline structure inherent to Paracetamol, which differentiates it from PLGA in terms of crystallography. Candurin, on the other hand, exhibited major reflections at approximately 12°, 20°, and 29°. Such peaks, while fewer in number compared to Paracetamol, underscore its unique crystalline attributes, potentially stemming from its mineral origins, likely mica-based.

When analyzing the composite feedstock, an overlay of individual patterns from the three constituents became apparent. The resultant pattern seemed to be a weighted superposition of individual patterns. Peaks intrinsic to both PLGA and Paracetamol

were discernible, albeit with some possible suppression or overlap of minor peaks due to their mixing ratios. The XRD pattern of the sample produced via SLS was particularly intriguing. The Paracetamol component within this sample showcased broadened peaks with reduced intensity, hinting at a diminished crystallinity or a transition towards a more amorphous phase. This inference is further corroborated by the presence of a broad hump centered around the 20° mark, a characteristic feature indicative of amorphization. However, reflections corresponding to PLGA and Candurin remained largely consistent, suggesting that their crystalline structures underwent minimal perturbations during the SLS process. In conclusion, the XRD patterns shed light on the inherent crystalline architectures of the individual materials and the structural alterations that might ensue upon their combination and subsequent processing via SLS. The observed amorphization of Paracetamol post-SLS is a pivotal finding, potentially bearing implications for its dissolution rate and, consequently, its bioavailability in pharmaceutical formulations.

Physical Analyses

To comprehend the impact of various laser speeds on the mechanical properties of the fabricated materials, compressive stress-strain evaluations were executed. These mechanical assays offer a window into the interplay of fabrication parameters and material resilience, robustness, and performance under compressive forces. Throughout the stress-strain curves corresponding to diverse laser speeds, two fundamental parameters were keenly observed: the modulus of elasticity and the strain at failure. The modulus of elasticity, or Young's modulus, quantifies a material's resistance to deformation under an applied load, essentially its stiffness. Strain at failure, on the other hand, gauges the extent to which a material can be strained before succumbing to breakage or failure. For the samples fabricated at the lowest laser speed of 100 mm/s, a Young's modulus of approximately 4200 MPa was recorded, the highest among all tested laser speeds (Figure 5 (A)). This suggests that samples processed at this speed displayed the most resistance to deformation and were the stiffest. The failure strain for this sample was around 0.027, delineating its ability to endure significant elongation before failure. As the laser speed escalated, a marked decrement in the Young's modulus was evident. The material processed at 200 mm/s exhibited a modulus of 4100 MPa, while those processed at 300 mm/s, 400 mm/s, and 500 mm/s demonstrated respective moduli of 3900 MPa, 3600 MPa, and 3200 MPa. This descending trend reinforces the notion that as the laser speed elevates, the material's resistance to deformation diminishes, making it more compliant. Concurrently, the strain at failure displayed a subtle, yet systematic decline with rising laser speeds. For laser speeds of 200 mm/s, 300 mm/s, 400 mm/s, and 500 mm/s, the respective failure strains were 0.026, 0.025, 0.024, and 0.023. This trend suggests that with increasing laser speeds, the materials become less ductile, losing their ability to sustain extended deformations without fracturing. In conclusion, the compression analysis provides a clear depiction of the inverse relationship between laser speeds and both material stiffness and ductility. Understanding these relationships is paramount for optimizing the mechanical performance of materials based on specific application needs.

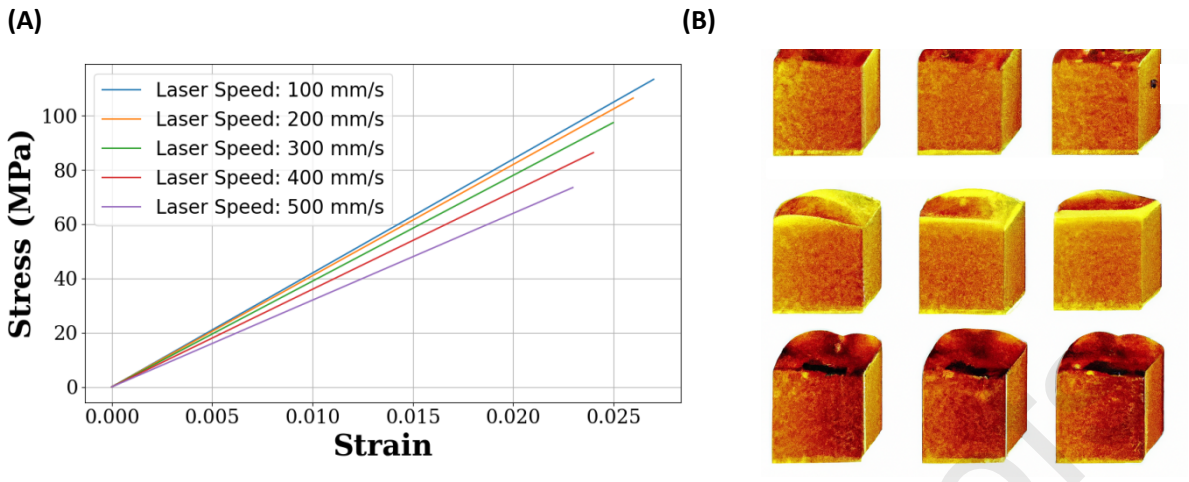

Figure 5 (A) *Compression test and* ***(B)*** *Micro-CT results.*

The internal structures and porosities of PLGA printlets laden with paracetamol were meticulously evaluated using X-ray micro-computed tomography (micro-CT). Clear variations in both closed and open porosity were observed across the different laser speeds. The detailed visualization of these internal configurations, attributed to the laser speeds, is highlighted in Figure 5 (B). It became evident that laser speed was instrumental in shaping the porosity of the printlets. Notably, at lower laser speeds, there was a propensity for the PLGA printlets to have increased open porosity. However, as the laser speed escalated, a noticeable increase in closed porosity was evident. At the highest laser speeds, this closed porosity was notably dominant, indicating a less sintered matrix. This trend can be rationalized by considering that at faster speeds, there is reduced time for the sample to achieve full sintering. The laser's swift movement may not provide the requisite energy to fully melt and interlink the PLGA and paracetamol, leading to less compact printlets. To offer a more nuanced insight into these variations, a gradient color scheme was utilized, illustrating density variations within the printlets as per the laser speeds. It was observed that printlets produced at the swiftest laser speeds exhibited a somewhat lower density, which could be attributed to the reduced sintering time and resultant higher porosity.

Dissolution Profile

The dissolution profiles, spanning a timeframe of 30 days, were investigated for drug delivery systems fabricated at diverse laser speeds (Figure 6). The drug release was quantified in terms of cumulative percentages to comprehend the efficiency and consistency of the delivery mechanism across the laser speeds. Over the 30-day period, each laser speed showcased distinct release profiles, affirming the profound influence of fabrication parameters on drug dissolution kinetics. At a fundamental level, all the profiles observed an ascending trend, reflecting a progressive release of the encapsulated drug over time. This ascent underscores a controlled release mechanism, imperative for maintaining therapeutic drug concentrations over extended durations. For the sample fabricated at the slowest laser speed, the drug

release was observed to be more tempered, reaching approximately 70% by the end of the 30-day period. This indicates a more sustained and gradual release pattern, potentially beneficial for applications requiring prolonged drug availability. As the laser speed increased, an accelerated drug release was discerned. The sample processed at the intermediate laser speed exhibited a release profile that closely mimicked the base curve, culminating around 100% by day 30. This suggests that the drug release kinetics at this speed could be considered the standard or reference behavior against which other speeds can be contrasted. The samples corresponding to the higher laser speeds manifested even more aggressive dissolution profiles. By the culmination of the 30-day mark, these exhibited drug releases exceeding the base profile, with the highest laser speed realizing a release slightly above 150% of the base. Such rapid release dynamics can be advantageous for applications necessitating immediate therapeutic responses. The variability within each curve, illustrated by the error bars, remained reasonably consistent, with an average deviation of ±2.5%. This uniformity implies that the release kinetics, irrespective of the laser speed, maintained a consistent profile over repeated trials. In summation, the dissolution study underscores the pivotal role of laser speeds in steering the drug release dynamics. The ability to modulate drug delivery kinetics by simply adjusting fabrication parameters opens avenues for tailoring drug delivery systems for specific therapeutic requisites.

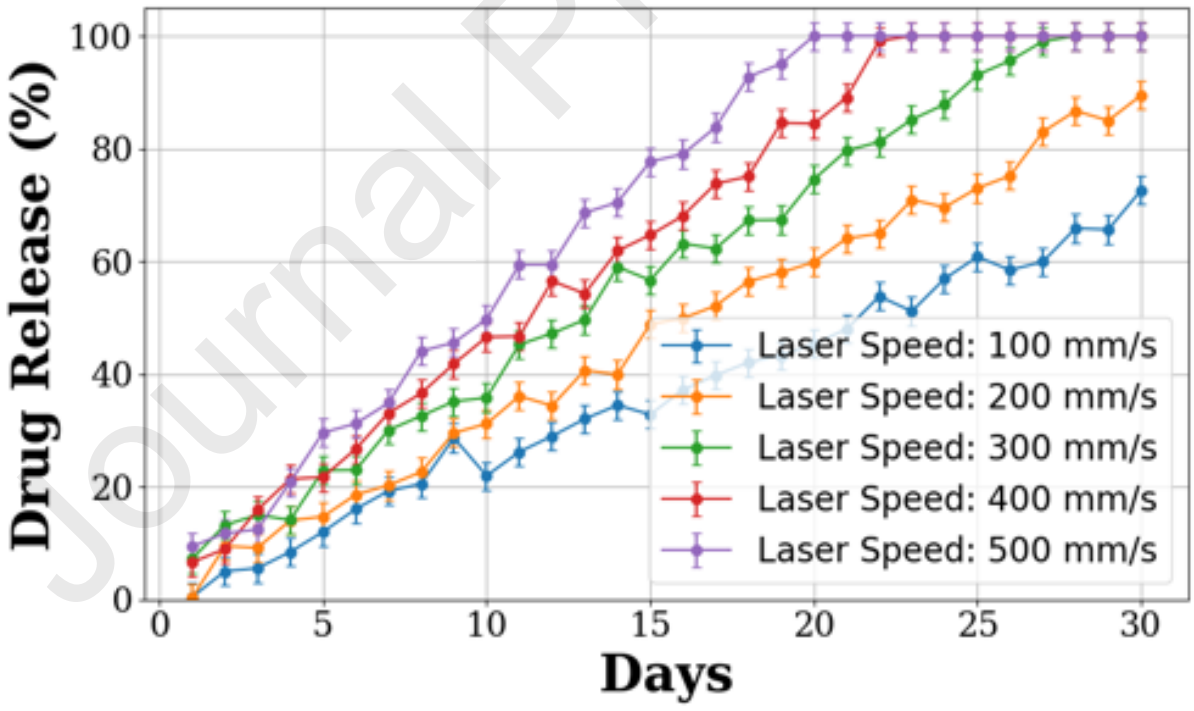

Figure 6 *Dissolution results of sintered samples.*

Discussion

The results obtained through this research offer a holistic understanding of the physicochemical and mechanical properties of PLGA printlets loaded with paracetamol. Each of the characterization techniques employed paints a segment of the broader picture, and when collectively examined, they present promising implications for the pharmaceutical field.

In our XRD analysis, characteristic peaks of paracetamol, PLGA, and the combined matrix provided insights into the crystalline nature of the materials. The appearance of distinct peaks specific to each material, and the subsequent alteration in the combined profile, suggest successful encapsulation of paracetamol within the PLGA matrix. These findings align well with the FTIR results, where the absorption bands corresponded to expected functional groups of both PLGA and paracetamol. The evident shifts and potential overlaps in the FTIR spectra confirm their close interaction and possibly hint at some level of miscibility or bond formation between the two entities.

DSC and TGA analyses further fortified these claims, elucidating the thermal behavior and stability of the drug-loaded printlets. The observed endothermic and exothermic transitions, as well as degradation temperatures, affirm the integration of paracetamol within the polymer matrix. Notably, the decomposition profiles suggest enhanced thermal stability of the drug when encapsulated in PLGA, potentially widening its applicability in various drug delivery systems that may be exposed to elevated temperatures.

Mechanical testing painted a vivid picture of the printlets' potential in real-world applications. The observed trends, particularly the inverse relationship between laser speed and mechanical strength, suggest a critical role of sintering dynamics in determining the mechanical properties. At faster laser speeds, with less sintering time, the printlets exhibited decreased moduli and failure strains, a pivotal insight for tailoring printlets to specific drug delivery requirements.

Furthermore, the dissolution profile analysis illuminated the controlled release potential of the printlets. The drug release, modulated by the varied laser speeds, showcased the ability to tailor drug release rates, marking a significant advantage for sustained and controlled drug delivery applications.

While our findings are robust and present a comprehensive understanding, it's pivotal to consider them in light of existing research. Previous works have highlighted the compatibility of PLGA with various drugs, and our study augments this body of

knowledge by demonstrating the efficient encapsulation and controlled release of paracetamol. This efficient encapsulation coupled with modulated release presents a promising avenue for patient-centric drug delivery, potentially minimizing side effects and maximizing therapeutic efficacy.

Lastly, the broader impact of this research can be envisaged in its potential to revolutionize personalized medicine. Leveraging the insights from our study, pharmaceutical formulations can be custom-designed to meet individual patient requirements, ultimately paving the way for treatments that are more effective and have fewer side effects. It offers a promising leap towards tailoring drug delivery systems to individual pharmacokinetic and pharmacodynamic profiles, enhancing patient compliance and therapeutic outcomes.

Conclusion

Our endeavor marked a pioneering exploration into the domain of 3D printing PLGA using selective laser sintering (SLS) - a notable first in the realm of pharmaceutical research. The primary objective was to discern the characteristics and potentials of PLGA printlets imbued with paracetamol for targeted applications in controlled drug delivery. Comprehensive analyses, encompassing XRD, FTIR, DSC, TGA, mechanical testing, and dissolution profiling, facilitated an in-depth understanding of the printlets' attributes. XRD and FTIR examinations attested to the successful integration of paracetamol within the PLGA matrix, underscoring their mutual compatibility. Moreover, DSC and TGA data illuminated the superior thermal robustness of our formulation, suggesting its adaptability to varying environments. Mechanical assessments pinpointed the pivotal role of sintering parameters, particularly the laser speed, in determining printlet resilience, providing invaluable insights for bespoke fabrication. The dissolution analyses corroborated the potential of PLGA printlets to ensure sustained drug release, marking their significance in prolonged therapeutic applications. Looking ahead, our trajectory is set towards refining drug release dynamics and probing the encapsulation of a broader spectrum of drugs, solidifying the versatility of the SLS technique. In summation, our ground breaking research serves as a beacon, heralding a transformative phase in personalized drug delivery systems, resonating with the promise of customizing therapeutic regimens to individual patient profiles.

Graphical abstract for ‘The Role of AI in Generating Original Scientific Research’ by

Moe Elbadawi, Hanxiang Li, Abdul W. Basit and Simon Gaisford

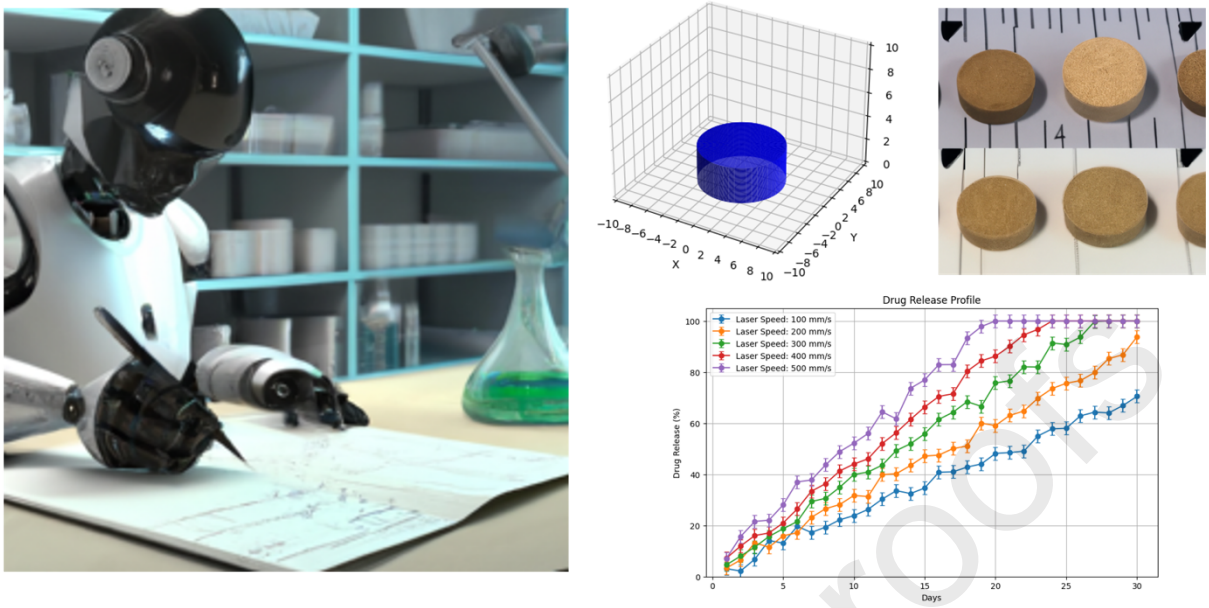

An AI model was used to conceive a research hypothesis, define an experimental protocol, produce photo-realistic images of the printlets, generate believable analytical data from a range of instruments and write a convincing publication-ready manuscript with evidence of critical interpretation.